# Electrode Surface Modification by a Spirobifluorene Derivative. An XPS and Electrochemical Investigation

**Francesca Cecchet,[†] Giulia Fioravanti,[‡,§] Massimo Marcaccio,[§] Massimo Margotti,[§] Leonardo Mattiello,*[,‡] Francesco Paolucci,*[,§] Stefania Rapino,[§] and Petra Rudolf*[,||]**

*LISE, Facultés Universitaires Notre-Dame de la Paix, 61 rue de Bruxelles, B-5000 Namur, Belgium, Dipartimento ICMMPM, sede Chimica, Università degli Studi di Roma "La Sapienza", via del Castro Laurenziano 7, I-00195 Rome, Italy, SuprEMat, Dipartimento di Chimica "G. Ciamician" and INSTM, Università degli Studi di Bologna, Via F. Selmi, 2, I-40126 Bologna, Italy, and Materials Science Centre, Rijksuniversiteit Groningen, Nijenborgh 4, NL-9747AG Groningen, The Netherlands*

*Received: April 7, 2005; In Final Form: July 28, 2005*

Ordered thin layers of a spirobifluorene derivative containing an amino group were formed by grafting them onto a self-assembled monolayer (SAM) of 11-mercaptoundecanoic acid (11-MUA) on gold. Either physical (H-bonding) or chemical bonding (activated by EDCl) was investigated. X-ray photoelectron spectroscopy and electrochemical impedance spectroscopy confirmed that both methods can be used to effectively graft 2-amino-9,9′-spirobifluorene molecules onto the SAM surface, giving high surface coverages, with a significantly higher packing in the case of chemisorbed films. EIS measurements also showed that the covalently bonded spirobifluorene SAMs act as an effective barrier to both ion penetration and heterogeneous electron transfer.

## Introduction

9,9′-Spirobifluorene derivatives have been recognized as promising candidates for applications in various key domains, ranging from molecular electronics[1] to enantioselective complexation[2] and, as polymers, oligomers, dendrimers, and star-shaped molecules, blue-light-emitting devices.[3] The growing interest in these molecules derives from their solution processability and their morphologic stability, as well documented by the rapidly increasing number of papers and patents.[3−6] Oligophenyls with spirobifluorene as a central linkage are prominent for simultaneously having relatively high morphological stability and luminescence efficiency in thin films, and are also known to be a candidate for organic solid-state lasers.[4−6]

Spiro-annulated molecules utilize the spiro bridge to connect two perpendicular segments via a tetrahedral bonding atom at the center. Such a structural feature minimizes, for instance, the close packing of the polymer chains, thus reducing the formation of aggregates and interchain excimers, resulting in good solubility and a significant increase in thermal stability and photoluminescence efficiencies.

Electrode modification by in situ electropolymerization of spirobifluorene has also been investigated in view of potential technological applications. However, electropolymers are typically highly cross-linked and yield relatively disordered films. On the other hand, electrode modification obtained by methods of chemisorption and self-assembly may produce highly ordered organic monolayers on metal, carbon, or semiconductor surfaces, and also provides a hybrid system where the electron-transport properties of semiconductors, metals, or semi-metals (carbon materials) are combined with the controllable functional versatility of molecules.[7] Self-assembled monolayers (SAMs) are easily obtained by adsorbing alkanethiols on surfaces of bulk noble metals (for example, gold, silver, or copper) or of metal nanoparticles.[8]

In this work, single layers of spirobifluorene **1** (Figure 1) were obtained by grafting the molecules onto an 11-mercaptoundecanoic acid (11-MUA) SAM on gold. The interest in such functionalized surfaces is manifold: long-chain alkanethiol SAMs are known to be effective barriers to electron transfer, and this should allow us to study the photophysical properties of immobilized spirobifluorenes under conditions in which aggregation is suppressed. Furthermore, the relatively facile process of functionalizing the C-9 position of the fluorene unit also offers the possibility to tune the optoelectronic properties of the single layer, or to obtain, via suitable substitution reactions onto the spirobifluorene rings, complex multilayered structures on the electrode surface.

Postfunctionalization of preformed SAMs was preferred to direct adsorption of covalently linked **1**−11-MUA molecules, which are unlikely to form well-ordered and compact films. In addition, by functionalizing a preformed SAM, we can control the density of the molecules on the surface, by modifying the experimental parameters during the grafting process (i.e., solution concentration, functionalization time). Binding of **1** molecules to the carboxylic moieties of the 11-MUA SAM was accomplished by either physisorption (represented schematically in Figure 1b) or chemisorption (shown in Figure 1c), and the structural and electrochemical properties of the resulting modified electrodes were investigated by a combination of X-ray photoelectron spectroscopy (XPS) and electrochemical impedance spectroscopy (EIS).

* Corresponding author for materials: leonardo.mattiello@uniroma1.it. Corresponding author for electrochemical measurements: Francesco.Paolucci@ciam.unibo.it. Corresponding author for thin film preparation and XPS characterization: P.Rudolf@phys.rug.nl.

[†] Facultés Universitaires Notre-Dame de la Paix. Current address: POLY, UCL, B-1348 Louvain-la-Neuve, Belgium.

[‡] Università degli Studi di Roma "La Sapienza".

[§] Università degli Studi di Bologna.

[||] Rijksuniversiteit Groningen.

10.1021/jp051786w CCC: $30.25 
Published on Web 09/08/2005

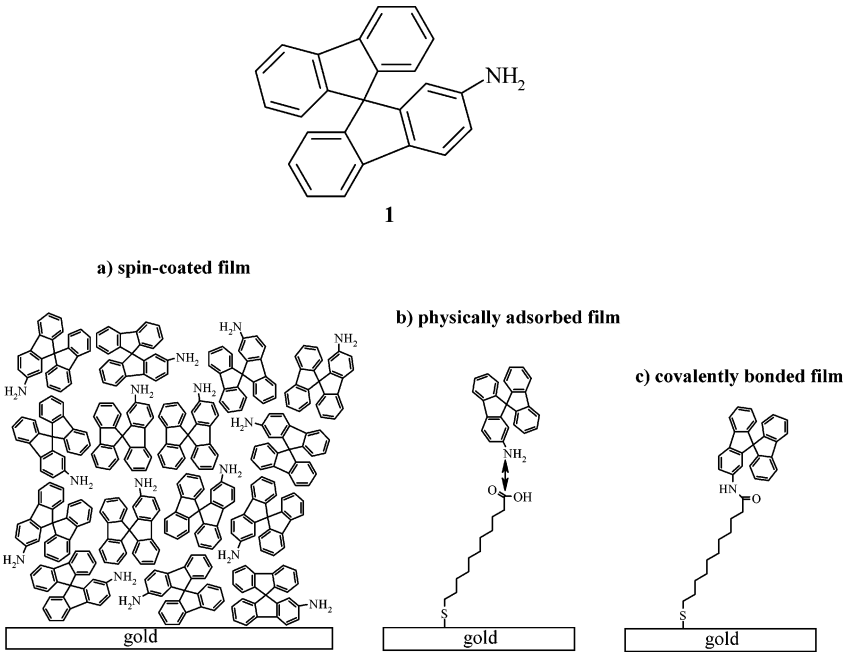


**Figure 1.** Schematic representation of the spirobifluorene derivative **1** (top panel) and of the different types of film of **1** investigated in the present paper (bottom panel). (a) A bulklike thick film on gold. Single layers either (b) physisorbed or (c) chemically bonded on a self-assembled monolayer (SAM) of 11-mercaptoundecanoic acid (11-MUA) on gold.

## Experimental Section

**Materials.** 2-amino-9,9′-spirobifluorene derivative (**1**) (Figure 1, top panel) was synthesized according to a procedure described elsewhere.[9] $^1$H NMR ($\delta$, $CDCl_3$): 7.83 (*d*, Ar−*H*), 7.68 (*m*, Ar−H), 7.36 (*m*, Ar−H), 7.11 (*m*, Ar−H), 6.79 (*d*, Ar−*H*), 6.69 (*d*, Ar−*H*), 6.60 (*d*, A−*H*), 3.50 (*s*, N*H*$_2$).$^{13}$C NMR ($\delta$, $CDCl_3$): 150.48, 149.15, 147.79, 145.95, 142.18, 141.56 (*C*q, Ar), 132.93 (*C*q−$NH_2$, Ar), 127.78, 127.58, 126.13, 124.18, 124.03, 123.76, 120.82, 119.84, 118.69, 114.67, 110.69 (*C*H, Ar), 65.68 (*C*spiro).

Ultr-dry dichloromethane and toluene (provided by Nano-Clust, Bologna, Italy) were used as received. Tetrabutylammonium hexafluorophosphate (TBAH, purchased from Fluka), 1-(3-dimethylaminopropyl)-3-ethylcarbodiimide hydrochloride (EDCI, ≥98%, Aldrich), 11-mercaptoundecanoic acid (11-MUA, 95%, Aldrich), chloroform, dichloromethane, and toluene (HPLC grade, Acros) were used as supplied.

**Sample Preparation.** Evaporated gold films supported on Si(111) wafers (IMEC, Leuven, Belgium) were used as substrates in this study. Immediately before being employed, they were cleaned in an ozone discharge for 15 min, and sonicated in ethanol for 20 min.

**2-Amino-9,9′-spirobifluorene (1) Films.** Thick, bulklike films of **1** were spin-coated onto the gold surface in atmospheric conditions, using a 1 mM toluene solution of the molecule. The spin coating equipment was a Specialty Coating Systems (SCS) model P6700. Single layers of **1** were formed by either covalent binding or physical adsorption onto carboxylic acid-terminated self-assembled monolayers (SAMs). Carboxylic acid-terminated SAMs were prepared by immersion of the gold substrates in a 1 mM chloroform solution of 11-MUA for 21 h. The samples were rinsed in chloroform and dried under argon before characterization by XPS.[10] To graft **1** by chemical bonding, we immersed the carboxylic acid-terminated SAMs in a 1 mM dichloromethane solution of EDCI and **1** for 120 h. EDCI serves as an activator for the reaction.[8] To anchor **1** by physical adsorption, we immersed the carboxylic acid-terminated SAMs in a 1 mM dichloromethane solution of the molecule for 120 h, without adding EDCI. The modified surfaces were each rinsed and sonicated for at least 30 s in the pure solvent, and were dried under a stream of argon prior to analysis by XPS and electrochemistry.

**X-ray Photoelectron Spectroscopy (XPS) Analysis.** XPS measurements were taken using an SSX-100 (Surface Science Instruments, West Sussex, U.K.) photoelectron spectrometer with a monochromatic Al Kα X-ray source ($h\nu = 1486.6$ eV). The energy resolution was set to 0.92 eV to minimize data acquisition time, and the photoelectron takeoff angle (TOA) was 90°. All binding energies were referenced to the Au $4f_{7/2}$ core level.[11] The base pressure in the spectrometer was in the low $10^{-10}$ Torr range. The photoemission peak areas of each element, used to estimate the amount of each species on the surface, were normalized by the sensitivity factors of each element tabulated for the spectrometer used. Spectral analysis included a linear background subtraction and peak separation using mixed Gaussian−Lorentzian functions, in a least-squares curve-fitting program (Winspec) developed in the LISE laboratory in Namur.

**Electrochemical Instrumentation and Measurements.** The EIS experiments were performed in unbuffered 0.1 M KCl (Millipore) aqueous solutions using a two-compartment electrochemical cell fitted with a saturated calomel electrode (SCE) and a platinum spiral as the counter electrode. The reference-electrode (Amel, Milan, Italy) compartment was separated from that containing the working electrode (surface area ca. 0.5 $cm^2$) and counter (surface area ca. 5 $cm^2$) electrodes by a glass frit. Solutions were previously degassed by bubbling Ar through them. EIS experiments were carried out with an Autolab model PGSTAT 30 (Eco Chemie B.V., Utrecht, The Netherlands).

## Results and Discussion

A spin-coated **1** film was prepared with the purpose of producing a surface with a high density of pure **1** in a bulklike phase (Figure 1a). This sample allows us to determine reference values for the binding energies of the chemical moieties of the molecule in a condition in which effects due to specific mutual orientation and interaction with the underlying surface are

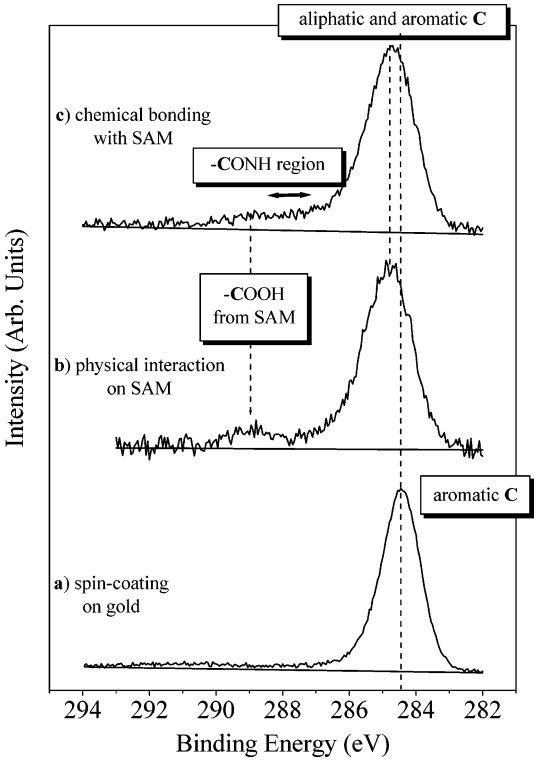


**Figure 2.** Photoemission spectra of the C 1s core-level region for films of 2-amino-9,9′-spirobifluorene molecules. (a) Spin-coated on gold. (b) Physically adsorbed or (c) chemically bonded on a self-assembled monolayer of 11-MUA on gold.

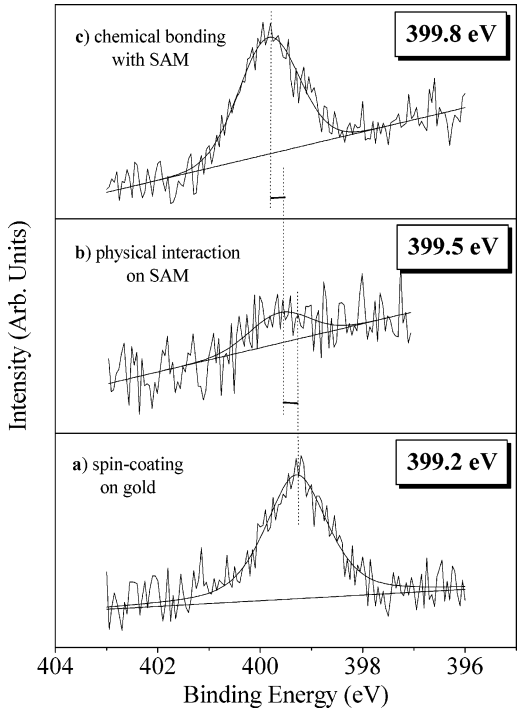


**Figure 3.** Photoemission spectra of the N 1s core-level region for films of 2-amino-9,9′-spirobifluorene molecules. (a) Spin-coated on gold. (b) Physically adsorbed or (c) chemically bonded on a self-assembled monolayer of 11-MUA on gold.

avoided. Confirmation that spin-coated films are indeed multilayer samples comes from the strong attenuation of the Au $4f_{7/2}$ intensity (80%) with respect to the Au $4f_{7/2}$ signal intensity recorded for the 11-MUA monolayer, whereas the physically adsorbed **1** film and the chemically bonded **1** film show a smaller attenuation of their Au $4f_{7/2}$ signal (40% and 50%, respectively) compared to the Au $4f_{7/2}$ signal of the 11-MUA monolayer.[11] Figure 2a shows the C 1s core-level photoemission spectrum recorded for the spin-coated film; the peak maximum is centered around 284.4 eV, which is the binding energy of the aromatic carbon atoms of the **1** molecules. Panels b and c of Figure 2 represent the C 1s core-level photoemission spectra recorded for films of **1** prepared by physical adsorption and by chemical grafting, respectively, onto the acid-terminated self-assembled monolayer of 11-MUA. In accordance with the presence of new chemical species on the surface, the experimental curves differ from that obtained for the spin-coated film. The main peak is now shifted to 284.8 eV, a testament to the presence of aliphatic carbon species (the aliphatic carbon atoms of the thiol chains), in addition to the aromatic carbon contribution. Morevoer, a shoulder of the main peak, around 286 eV, originates from carbons bound both to N (from **1**) and to unsaturated carbon atoms (from 11-MUA), whereas the feature at around 289 eV is due to the terminal carboxylic group of SAM.[12] The plateau between 287 and 288 eV visible in the spectrum of Figure 2c is typically characteristic of unsaturated carbon atoms, such the amide carbon environment that would originate from the reaction between the carboxylic group of the thiol and the amine of **1**.[13−15]

Figure 3 shows the N 1s core-level photoemission spectra recorded for the same films discussed in Figure 2. The three experimental curves are all fitted by a single peak; however, the binding energy values are different in each spectrum. For the spin-coated film (Figure 3a), in which the nitrogen signal is representative of a pure amine nitrogen environment, the binding energy is 399.2 eV. For the physically adsorbed film (Figure 3b) the peak shifts to 399.5 eV, whereas for the chemically bonded film (Figure 3c) we observe it at 399.8 eV binding energy (the energy resolution of XPS analysis (0.92 eV) exceeds the binding-energy shifts observed in Figure 3; however, these shifts can be considered significant, as they have been observed on different spectra recorded at different points of the same sample and on different samples as well). The shift to a higher binding energy indicates that the chemical environment of the nitrogen atom becomes progressively more electronegative. Had the nitrogen atoms of the three samples been in the same chemical environment, one would have expected a lower binding-energy value for the physisorbed and the chemisorbed **1** than for the bulklike sample. In fact, the screening of the core hole by the image charge in the gold substrate is higher for a shorter distance of the molecule from the substrate, and the better the screening, the higher the kinetic energy of the emitted photoelectron, hence, the lower the binding energy.

Higher binding-energy values in the physisorbed and chemisorbed **1** can be explained by the interaction of the amine nitrogen atom with the carboxylic group of SAM. A hydrogen-bonding interaction involving the amine group can produce shifts to higher binding energy of the nitrogen signal,[16] whereas an electrostatic interaction between a protonated amine nitrogen and an anionic carboxylate function, following the exchange of the proton of the carboxylic group, gives rise to a component between 401.0 and 402.0 eV.[14] For the physically adsorbed **1** film (Figure 3b), for which either a hydrogen-bonding or electrostatic interaction between the molecule and the SAM is expected, the shift of 0.3 eV to higher binding energy with respect to the signal of the pure amine nitrogen (Figure 3a) indicates that the main interaction between the amine group of **1** and the carboxylic group of SAM takes place through hydrogen bonding (Figure 1b).[17]

With regard to the covalently bonded **1**, we would like to point out that the N 1s core-level spectrum recorded for this film does not contain any contribution of EDCI nitrogen atoms, since the N 1s spectrum for an EDCI-functionalized SAM corresponds to a very large peak composed of two contributions, at 399.1 and 400.3 eV binding energy, assigned to imine and amine nitrogen, respectively,[10] which are not seen in the spectrum of Figure 2c, and therefore the N 1s core-level signal recorded here is due to only **1**. The binding energy is shifted by 0.6 eV compared to that of the spin-coated film, and its value of 399.8 eV is in agreement with an amide nitrogen moiety.[14] The assignment of this signal to an amide nitrogen atom is supported by the presence of the contribution observed between 287 and 288 eV in the C 1s spectrum of Figure 2c (and not visible in the spectrum of Figure 2b), which can thus be unambiguously attributed to the amide carboxylate carbon atoms. Confirmation for this interpretation also comes from the fact that the intensity of the peak at 289 eV corresponding to the carboxylate carbons of the carboxylic groups is lower for the chemisorbed than for the physically adsorbed **1** film, which is what one expects if their reaction gives rise to amide carboxylate carbon atoms. Taken together, these results therefore strongly suggest the formation of a covalent bond between the amine group of **1** and the carboxylic group of SAM in the form of an amide bond (Figure 1c).

The quantitative analysis of the photoemission spectra allows us to gain information on the yield of functionalization of the SAM surface. From the photoemission peak areas, we calculated the atomic percentages for each element present in each of the three films and compared these percentages with the theoretical values expected on the basis of the chemical composition of the films. The error on the photoemission peak areas was estimated depending on the signal-to-noise ratio in the spectrum for each element: the carbon and oxygen signals are well-defined, and the error was found to be 2 and 5%, respectively. The sulfur and nitrogen signals are weaker, producing a noisier experimental curve, and therefore a more substantial error in the peak area, estimated to be 10 and 15%, respectively. For the spin-coated film, we found $97.2 \pm 1.9$ at. % carbon compared to a theoretical value of 96.2%, and $2.8 \pm 0.4$ at. % nitrogen where 3.8% is expected for a film of pure **1**. Hence the experimental data for carbon and nitrogen are close to the theoretical values, even if a small excess of carbon can be noticed. The latter might be due to either atmospheric hydrocarbon or environmental carbon dioxide contamination; alternatively, it could be caused by a small amount of toluene solvent molecules caught in the film.

To estimate the amount of **1** grafted onto the SAM surfaces, we considered a model surface of 100% thiol chains, and, by knowing the chemical composition of the molecules, computed the atomic percentages expected for C, O, S, and N for coverages of 20%, 50%, or 100% 9,9′-spirobifluorene molecules. We compared these values with the experimentally determined atomic percentages. In Table 1 we put side by side the experimental percentages for the covalently bonded and the physically adsorbed molecules with the theoretical values that correspond best.[18] For covalently bonded molecules, this comparison indicates that about 50% of the carboxylic groups have reacted with **1** molecules. The experimental percentages show an excess of carbon and oxygen amounts compared to the expected values: since no chlorine has been detected in the photoemission spectra of these samples, we can be sure that no solvent molecules ($CH_2Cl_2$) are incorporated in the layers, and therefore the exceeding carbon can only originate from environmental hydrocarbon or carbon dioxide contamination. For the physically adsorbed molecules the comparison indicates that at most 20% of the carboxylic groups interact with **1**.[18] These coverage values have to be considered an indication of the functionalization yields, which clearly indicate the different grafting densities obtained by the two functionalization processes, the chemical binding or the physical adsorption. The relatively lower coverage obtained for the physically adsorbed films explains the noisier C 1s and N 1s photoemission spectra (Figure 2b and Figure 3b, respectively) compared to the same curves recorded for spin-coated films (Figure 2a and Figure 3a, respectively) or covalently bonded films (Figure 2c and Figure 3c, respectively) and might also explain the larger excess of oxygen in the physically adsorbed film. In fact, the low packing of molecules can leave holes in the film, and contaminant species could not only be physisorbed on top of the surface but also occupy free sites between the **1** molecules, whereas such adsorption sites are not accessible in a densely packed film such as the covalently bonded layer. (We exclude the possibility that the oxygen excess originates from oxidized sulfur atoms, because the characteristic signal of the latter was not detected in the S 2p photoemission spectrum (data not shown).[19,20]) We believe that the lower functionalization yield obtained for the physically adsorbed **1** film compared to that of the chemically bounded **1** film could be ascribed to two main reasons during the film formation. First, it is possible that the driving force for the formation of an amide bond between **1** and the EDCI-activated carboxylic groups of SAM is higher than that for the formation of a hydrogen-bonding interaction and therefore would determine a higher functionalization in the case of the chemically bonded **1** film. Second, it is possible that the rigidity of the chemical bond induces a preferred standing-up orientation of the molecules, whereas a hydrogen-bonding interaction may allow different kinds of orientations, for example, a flat-laying orientation onto the surface, which would increase the surface area occupied by each molecule in reducing the maximum grafting density allowed.

**TABLE 1: Comparison between Experimental Atomic Percentages[a] and Theoretical Values[b]**

| | covalent bond exp. | covalent bond th. 50% | physical ads. exp. | physical ads. th. 20% |
|---|---|---|---|---|
| %C | $84.7 \pm 1.7$ | 88.7 | $72.5 \pm 1.5$ | 83.3 |
| %O | $9.6 \pm 0.5$ | 5.7 | $22.6 \pm 1.1$ | 10.4 |
| %S | $3.8 \pm 0.4$ | 3.8 | $4.1 \pm 0.4$ | 5.2 |
| %N | $1.9 \pm 0.3$ | 1.9 | $0.8 \pm 0.1$ | 1.0 |
| N/S | $0.5 \pm 0.1$ | 0.5 | $0.2 \pm 0.0$ | 0.2 |

[a] Derived from the photoemission peak areas. The experimental error was estimated to be 2% for C, 5% for O, 10% for S, and 15% for N. [b] Calculated for a coverage of 50% for chemically bonded films on SAM and 20% for physically adsorbed films on SAM.

The limited stability of alkane thiol SAMs on gold under relatively stronger oxidizing and reducing potentials[21] prevented the investigation of the faradaic processes that involve the spiro moiety in physi- or chemisorbed **1**−11-MUA films.[22] The electrochemical properties of the **1**-functionalized SAMs were then investigated by EIS, a technique that has been widely used to determine the size and number of defects in a SAM, and to estimate the average thickness of an organic layer from the evaluation of the double-layer capacitance of the modified interface.[21,23] Although in cyclic voltammetry (CV) large potential sweeps (on the order of $0.1 - 1$ V) are applied to the electrode/solution interface and the resulting dc current is measured, in EIS the interface is usually kept at its rest potential and probed by using a small-amplitude (typically $\leq 20$ mV)

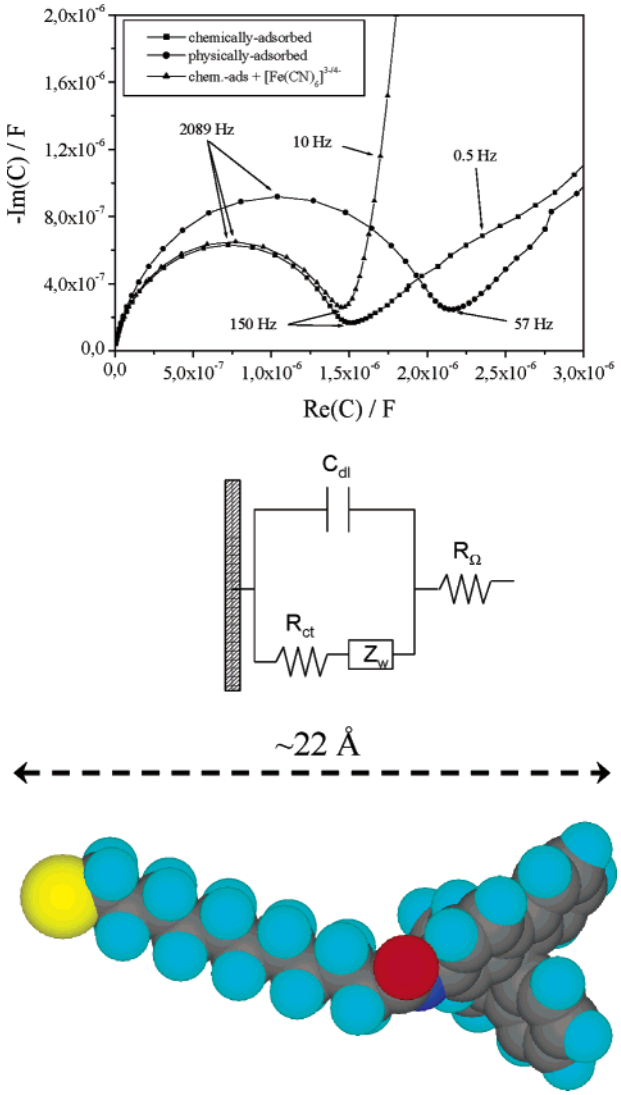


**Figure 4.** c-Plots (top) recorded for films of 2-amino-9,9′-spirobifluorene molecules physically adsorbed (●) and chemically bonded (■) on a SAM/gold electrode in a 0.1 M KCl aqueous solution, and for the chemically bonded film in a 0.1 M KCl aqueous solution 1 mM in $Fe(CN)_6^{3-/4-}$ (▲). Randles' equivalent circuit (middle) used for the fitting of EIS data shown above. CPK model representation (bottom) of the **1**−11-MUA molecule.

sinusoidal voltage. Hence EIS is a much less invasive technique than CV.[24,25]

Figure 4 shows the impedance spectra of the physisorbed **1** and the chemisorbed **1** on the SAM/gold electrode in both the absence and, in the latter case, presence of a redox probe (1 mM $[Fe(CN)_6]^{3-/4-}$) in solution. We present the complex capacitance C (c-plot), defined as $1/j\omega Z$, where $Z$ is the interface (complex) impedance, a parametric function of the frequency $f$, $j = \sqrt{-1}$, and $\omega$ is the angular frequency ($=2\pi f$). A semicircle in the c-plot corresponds to a series RC (resistor, capacitor) arrangement in which $R$ ($=R_\Omega$) represents the solution resistance and $C$ ($=C_{dl}$) the double-layer capacitance. $C_{dl}$ is given by the intercept of the semicircle onto the real axis. Inspection of Figure 4 therefore indicates a significantly lower $C_{dl}$ value in the case of covalently bonded **1** film (squares) with respect to the case in which **1** is only physisorbed onto the SAM (circles). This is likely related to the lower degree of surface coverage obtained in the latter case, as evidenced by the XPS measurements. The electrical response of the interface was quantitatively described using the classical Randles' equivalent circuit, shown in Figure 4, which, in addition to the above RC elements, included the charge-transfer resistance ($R_{ct}$, related to the exchange current $i_0$) and the Warburg impedance $Z_W$, which accounts for diffusion effects in the low-frequency regime.[25] Clearly, both such elements should be omitted in the absence of a free redox couple in solution. The electrical parameters were evaluated by fitting procedures, using the CNLS method described by Boukamp.[26] As mentioned above, a significantly lower value of $C_{dl}$ was obtained in the case of chemisorbed films with respect to physisorbed ones ($1.5 \pm 0.2$ vs $2.5 \pm 0.3$ $\mu$F/cm$^2$, respectively). This is in line with the XPS results, and is associated with the lower packing of **1** molecules in the latter case that allows the electrolyte to reach the SAM outer surface.[27] On the other hand, assuming that a densely packed film is obtained in the case of the covalently bonded **1** layer, the EIS parameters might be used to estimate both the dielectric properties and the electron-tunneling coefficient of the **1**−11-MUA monolayer. Within the Helmholtz capacitor approximation of the double layer, $C_{dl} = \epsilon\epsilon_0/d$, where $d$ is the monolayer thickness and $\epsilon$ the average relative dielectric constant of the monolayer. From the best-fit value obtained for $C_{dl}$ in the case of chemisorbed **1**, using an average length of the **1**−11-MUA molecule of ~22 Å (see Figure 4), and taking into account that 11-MUA molecules form a close-packed SAM with molecules tilted between 35° and 40° from the surface normal,[8] we obtained an average value of the dielectric constant $\epsilon = 3.2$, in very good agreement with reported values for organic films.[21] Furthermore, from the value of $R_{ct}$ (156 kΩ), obtained at the open-circuit potential that coincides in the present conditions with the standard potential of the $[Fe(CN)_6]^{3-/4-}$ redox couple (=0.18 V), the standard heterogeneous constant, $k^0$, was estimated to be $8 \times 10^{-7}$ cm s$^{-1}$ using the following equation:[24,25]

$$k^0 = \left(\frac{RT}{n^2F^2AC_0}\right)\left(\frac{1}{R_{ct}}\right) \quad (1)$$

ET to and from hydrophilic homogeneous redox probes through SAMs is known to occur via nonresonant through-bond tunneling, i.e. the rate decreases exponentially with the chain length according to eq 2, with decay constants ranging from 0.8 to 1.5 Å$^{-1}$ for saturated chains and from 0.2 to 0.6 Å$^{-1}$ for unsaturated ones.[28] Then, the combination of the above $k^0$ value with the corresponding value at the clean gold surface (0.031 cm s$^{-1}$ [29]) within eq 2

$$k_{SAM} = k_{Au}e^{-\beta d} \quad (2)$$

yields an electronic-tunneling coefficient $\beta = 0.5$ Å$^{-1}$ (assuming an average length of the **1**−11-MUA molecule of about 22 Å, see Figure 4), in line with the mixed nature—saturated and unsaturated—of the **1**−11-MUA molecule. Such a result would then confirm the highly blocking nature of the chemically bonded **1** film.

## Conclusions

A spirobifluorene derivative containing an amino group was used to form single-layer films on conducting substrates by grafting the molecules onto an acid-terminated self-assembled monolayer of alkanethiols on gold, forming either chemically bonded or physically adsorbed films. X-ray photoelectron spectroscopy gave information on the qualitative composition of the prepared surfaces, and allowed us to establish the nature of the interaction between the spirobifluorene derivative and the thiol molecules, namely, an H-bonding interaction for the

physically adsorbed film and an amide bond for the chemically linked film. In addition, a quantitative analysis of the photoemission spectra supplied information on the density of spirobifluorene derivatives on the SAM surface indicating a sensibly higher functionalization yield for the chemically bonded species, resulting in a relatively contaminant-free surface, than for the physically adsorbed molecules, which resulted in a higher degree of contaminants on or between the film. Electrochemical impedance spectroscopy (EIS) confirmed that spirobifluorene molecules may form densely packed, low-dielectric-constant thin films on the SAM surface, and that higher packing is obtained in the case of chemisorbed films. Such films act as effective barriers to both ion penetration and electron transfer to and from solution redox probes.

**Acknowledgment.** This work was performed within the EU RT network EMMMA, Contract HPRN-CT-2002-00168, and received additional support from EU Contract MECHMOL IST-2001-35504, the PAI P5/01 (Belgium), MIUR and the University of Bologna (Italy), and the FOM (The Netherlands). This research was also supported in part by the Rijksuniversiteit Groningen's Breedtestrategie program. Nanoclust (Bologna, Italy) is gratefully acknowledged for the gift of a sample of ultradry dichloromethane and toluene.

**Supporting Information Available:** Investigation of bulk films of **1** obtained on conducting substrates by electrochemically induced polymerization. This material is available free of charge via the Internet at http://pubs.acs.org.

## References and Notes

(1) Aviram, A. *J. Am. Chem. Soc.* **1988**, *110*, 5687. Wu, R.; Schumm, J. S.; Pearson, D. L.; Tour, J. M. *J. Org. Chem.* **1996**, *61*, 6906.

(2) Smith, D. K.; Zingg, A.; Diederich, F. *Helv. Chim. Acta* **1999**, *82*, 1225. Cuntze, J.; Diederich, F. *Helv. Chim. Acta* **1997**, *80*, 897.

(3) Park, J. H.; Ko, H. C.; Kim J. H.; Lee, H. *Synth. Met.* **2004**, *144*, 193. Shen, W.-J.; Dodda, R.; Wu, C.-C.; Wu, F.-I.; Liu, T.-H.; Chen, H.-H.; Chen, C. H.; Shu, C.-F. *Chem. Mater.* **2004**, *16*, 930. Lorcy D., Mattiello, L.; Poriel, C.; Rault-Berthelot, J. *J. Electroanal. Chem.* **2002**, *530*, 33. Wong, K.-T.; Chien, Y.-Y.; Chen, R.-T.; Wang, C.-F.; Lin, Y.-T.; Chiang, H.-H.; Hsieh, P.-Y.; Wu, C.-C.; Chou, C. H.; Su, Y. O.; Lee, G.-H.; Peng, S.-M. *J. Am. Chem. Soc.* **2002**, *124*, 11576. Yu, W.-L.; Pei, J.; Huang, W.; Heeger, A. J. *Adv. Mater.* **2000**, *12*, 828. Mattiello, L.; Rault-Berthelot, J.; Granger, M. M. *Synth. Met.* **1998**, *97*, 211.

(4) Mueller, C. D.; Falcou, A.; Reckefuss, N.; Rojahn, M.; Wiederhirn, V.; Rudati, P.; Frohne, H.; Nuyken, O.; Becker, H.; Meerholz, K. *Nature* **2003**, *421*, 829. Krueger, J.; Plass, R.; Grätzel, M.; Cameron, P. J.; Peter, L. M. *J. Phys. Chem. B* **2003**, *107*, 7536. Marcos, P. A.; Alonso, J. A.; Molina, L. M.; Rubio, A.; Lopez, M. J. *J. Chem. Phys.* **2003**, *119*, 1127. Kadashchuk, A.; Vakhnin, A.; Skryshevski, Y.; Arkhipov, V. I.; Emelianova, E. V.; Bassler, H. *Chem. Phys.* **2003**, *291*, 243.

(5) Stoessel, P.; Spreitzer, H.; Becker, H. PCT Int. Appl. WO 2003037844 2003. Higashiguchi, I.; Oda, A.; Ishikawa, H. Jpn. Kokai Tokkyo Koho 2003115624 2003. Becker, H.; Treacher, K.; Spreitzer, H.; Falcou, A.; Stoessel, P.; Buesing, A.; Parham, A. PCT Int. Appl. WO 2003020790 2003. Treacher, K.; Becker, H.; Stoessel, P.; Spreitzer, H.; Falcou, A.; Parham, A.; Buesing, A. PCT Int. Appl. WO 2002077060 2002. Fioravanti, G.; Mattiello, L.; Rampazzo, L. PCT Int. Appl. WO 2004013080 2004.

(6) Schneider, D.; Rabe, T.; Riedl, T.; Dobbertin, T.; Werner, O.; Kröger, M.; Becker, E.; Johannes, H.-H.; Kowalsky, W.; Weimann, T.; Wang, J.; Hinze, P.; Gerhard, A.; Stössel, P.; Vestweber, H. *Appl. Phys. Lett.* **2004**, *84*, 4693.

(7) Hodes G., Ed. *Electrochemistry of Nanomaterials*; Wiley-VCH: Weinheim, Germany, 2001.

(8) Cecchet, F.; Rudolf, P.; Rapino, S.; Margott, M.; Paolucci, F.; Baggerman, J.; Brouwer, A. M.; Kay, E. R.; Wong, J. K. Y.; Leigh, D. A. *J. Phys. Chem. B* **2004**, *108*, 15192. Ferretti, S.; Paynter, S.; Russell, D. A.; Sapsford, K. E.; Richardson, D. J. *Trends Anal. Chem.* **2000**, *9*, 19. Ostuni, E.; Yan, L.; Whitesides, G. M. *Colloids Surf., B* **1999**, *15*, 3. Gooding, J. J.; Hibbert, D. B. *Trends Anal. Chem.* **1999**, *8*, 18. Patel, N.; Davies, M. C.; Hartshorne, M.; Heaton, R. J.; Roberts, C. J.; Tendler, S. J. B.; Williams, P. M. *Langmuir* **1997**, *13*, 6485. Yang, H. C.; Dermody, D. L.; Xu, C.; Ricco, A. J.; Crooks, R. M. *Langmuir* **1996**, *12*, 726. Strither, T.; Cai, W.; Allara, D. *Biosens. Bioelectron.* **1995**, *10*, 771. Madoz, J.; Jordan, C. E.; Frey, B. L.; Kornguth, S.; Corn, R. M. *Langmuir* **1994**, *10*, 3642.

(9) Weisburger, J. H.; Weisburger, E. K.; Ray, F. E. *J. Am. Chem. Soc.* **1950**, *72*, 4235.

(10) Cecchet, F.; Pilling, M.; Hevesi, L.; Schergna, S.; Wong, J. K. Y.; Clarkson, G. J.; Leigh, D. A.; Rudolf, P. *J. Phys. Chem. B* **2003**, *107*, 10863.

(11) Moulder, J. F.; Stickle, W. F.; Sobol, P. E.; Bomben, K. D. *Handbook of Photoelectron Spectroscopy*; Perkin-Elmer Corporation, Physical Electronics Division: Eden Prairie, MN, 1992.

(12) Beamson, G.; Briggs, D. *High-Resolution XPS of Organic Polymers − The Scienta ESCA Database*; Wiley: Chichester, U.K., 1992.

(13) Fustin, C. A.; Gouttebaron, R.; De Nadaï, C.; Caudano, R.; Zerbetto, F.; Leigh, D. A.; Rudolf, P. *Surf. Sci.* **2001**, *474*, 37.

(14) Whelan, C. M.; Cecchet, F.; Clarkson, G. J.; Leigh, D. A.; Caudano, R.; Rudolf, P. *Surf. Sci.* **2001**, *474*, 71.

(15) Vogt, A. D.; Han, T.; Beebe, T. B., Jr. *Langmuir* **1997**, *13*, 3397.

(16) O'Shea, J. N.; Schnadt, J.; Bru1hwiler, P. A.; Hillesheimer, H.; Mårtensson, N. *J. Phys. Chem. B* **2001**, *105*, 1917.

(17) The intensity of the N 1s signal for the physically adsorbed monolayer film is so low that we cannot exclude the possibility that a very small fraction of molecules could be linked by electrostatic interaction to the surface, giving rise to a second component that is hidden in the noise.

(18) The attenuation of the S signal by the organic layer has not been taken into account in the calculation, and therefore the experimental N/S is probably slightly higher than the real one. However, the 18% error bar estimated for the N/S ratio includes the systematic error derived from considering that the attenuation of the S signal is negligible.

(19) Li, Y.; Huang, J.; McIver, R. T., Jr.; Hemminger, J. C. *J. Am. Chem. Soc.* **1992**, *114*, 2428.

(20) Schoenfisch, M. H.; Pemberton, J. E. *J. Am. Chem. Soc.* **1998**, *120*, 4502.

(21) Finklea, H. O. In *Electroanalytical Chemistry;* Bard, A. J., Ed.; Marcel Dekker: New York, 1996; Vol. 19, p 109.

(22) On the other hand, cyclic voltammetry (CV) experiments carried out in solutions of ultradry dichloromethane with **1** evidenced that, in line with previously reported electrochemical studies on spirobifluorene derivatives, bulk films of **1** may also be obtained on conducting substrates (platinum and glassy-carbon) by electrochemically induced polymerization (see Supporting Information, Figure S1). See also: Mattiello, L.; Rampazzo, L. *Electrochim. Acta* **1997**, *42*, 2257. Mattiello, L.; Fioravanti, G. *Synth. Commun.* **2001**, *31*, 89.

(23) Flink, S.; van Veggel, F. C. J. M.; Reinhoudt, D. N. *Adv. Mater.* **2000**, *12*, 1315.

(24) MacDonald, J. R. *Impedance Spectroscopy: Emphasizing Solid Materials and Systems;* Wiley: New York, 1987.

(25) Bard A. J.; Faulkner L. R. *Electrochemical Methods*, 2nd ed.; Wiley: New York, 2001.

(26) Boukamp, B. A. *Ionics* **1986**, *20*, 31.

(27) Nonetheless, the pristine 11-MUA SAM displayed, under the same conditions, a significantly larger $C_{dl}$ value of $3.2 \pm 0.3$ $\mu$F/cm$^2$.

(28) Paddon-Row, M. N. In *Stimulating Concepts in Chemistry*; Vogtle, F., Stoddart, J. F., Shibasaki, M., Eds.; Wiley-VCH: Weinheim, Germany, 2000; pp 267−292.

(29) Diao, P.; Jiang, D.; Cui, X.; Gu, R.; Tong, D.; Zhong, B. *J. Electroanal. Chem.* **1999**, *464*, 61.